

# Design, Synthesis, and Conformational Analysis of a Proposed Type I $\beta$ -Turn Mimic

Brian E. Fink, Phil R. Kym,<sup>†</sup> and John A. Katzenellenbogen\*

Contribution from the Department of Chemistry, University of Illinois, 600 S. Mathews Avenue, Urbana, Illinois 61801

Received November 25, 1997

**Abstract:** In an effort to design a dipeptide structural mimic of protein and peptide  $\beta$ -turns, we have prepared and evaluated the conformation of derivatives of the novel, highly constrained ten-membered lactam, (3*S*,10*S*)-(6*E*)-2-azacyclodec-6-enone (**1**). A synthetic route utilizing ring-closing olefin metathesis (RCM) has been used to prepare this novel ten-membered ring in high yield. X-ray crystallography and <sup>1</sup>H NMR analysis have established that ring closure proceeds to give the *trans*-olefin and that **1** exists in two conformations, that of a chair–chair and chair–boat. Monte Carlo-molecular mechanics conformational searching has indicated that this ring system would be a good mimic of a type I  $\beta$ -turn. The synthesis of model tri- and tetrapeptide analogues based on **1** is reported. NMR studies indicate that the tetrapeptide derivatives constrain the *i*+1 and *i*+2 torsion angles to within 30° of those predicted for an ideal type I  $\beta$ -turn ( $\phi_1 = -82^\circ$ ,  $\psi_1 = -20^\circ$ ,  $\phi_2 = -107^\circ$ ,  $\psi_2 = -18^\circ$ ) and that this conformation was shown to be stable in both hydrogen-bonding solvents as well as non-hydrogen bonding solvents at various temperatures.

## Introduction

Peptide ligands and protein receptors play critical roles in the regulation of nearly every biological process. Despite this central role, identifying the basic elements necessary for recognition between a peptide ligand and its receptor at the molecular level remains a formidable task. While advances in site-directed mutagenesis and peptide synthesis have provided dramatic insights into the functional group requirements for binding, they offer little information regarding the spatial orientation of both ligand and receptor upon binding. Knowledge of the intimate details of the three-dimensional interaction between peptide ligand and protein receptor could be invaluable in understanding bioactivity and in the design of analogues during the drug discovery process.

In most cases, determining the spatial orientation of important functionality has involved the conformational analysis of the native peptide ligand using such techniques as NMR spectroscopy, X-ray crystallography, circular dichroism, and molecular modeling.<sup>1,2</sup> However, peptides are characteristically highly flexible molecules that exist in multiple conformations. The central issue is then whether the conformation found in solution has any real physical meaning or whether it represents an average of the numerous conformations available to the peptide. Perhaps the more important question is whether any of these solution conformations correspond to that which is adopted by the peptide ligand when it is bound to the receptor.<sup>3</sup> While

great strides have been made, the direct determination of the receptor-bound conformation adopted by a bioactive peptide is still a formidable endeavor.

One method for the indirect determination of the bioactive conformation of a peptide ligand is through the implementation of conformational restrictions which limit the torsional space available to the native peptide.<sup>3,4</sup> A highly flexible molecule undergoes a large loss in entropy upon binding its receptor. However, an analogue of the native peptide which properly restricts important recognition elements to an appropriate three-dimensional geometry should experience less of an entropic change and may thereby bind more effectively to a receptor than its more flexible natural counterpart.<sup>4</sup> In this way, conformationally restricted peptides offer a means to probe peptide ligand conformation and provide indirect information about the three-dimensional interplay between receptor and ligand. In the pursuit of this strategy, many efforts have been made to prepare compounds that mimic certain secondary structural features of peptides which are thought to play important roles in recognition and biological activity.<sup>3–5</sup>

One common structural feature observed in small peptides and proteins is the  $\beta$ -turn (Figure 1).<sup>1</sup> By definition, the  $\beta$ -turn consists of a tetraresidue sequence in which the peptide chain reverses direction by approximately 180°. Most  $\beta$ -turns contain an intramolecular hydrogen bond between the carbonyl oxygen of the first residue (*i*) and the amide NH proton of the fourth residue (*i*+3), which forms a pseudo-ten-membered ring (Figure 1).  $\beta$ -Turns that do not show an intramolecular hydrogen bond are termed as “open turns”.<sup>1,7</sup> Of the most commonly found  $\beta$ -turns (see below), approximately 60% show an intramolecular hydrogen bond.<sup>4</sup>

\* Address correspondence to John A. Katzenellenbogen, Department of Chemistry, University of Illinois, 461 Roger Adams Laboratory, Box 37-5, 600 S. Mathews Avenue, Urbana, IL 61801. Telephone: (217) 333-6310. Fax: (217) 333-7325. E-mail: jkatzene@uiuc.edu.

<sup>†</sup> Current address: Abbott Laboratories, Department 4NB, Bldg. AP10, 100 Abbott Park Road, Abbott Park, IL 60064.

(1) Smith, J. A.; Pease, L. G. *CRC Crit. Rev. Biochem.* **1980**, *8*, 314–398.

(2) Rose, G. D.; Gierash, L. M.; Smith, J. A. *Adv. Prot. Chem.* **1985**, *37*, 1–109.

(3) Hruby, V. *Life Sci.* **1982**, *31*, 189–199.

(4) Ball, J. B.; Alewood, P. F. *J. Mol. Recogn.* **1990**, *3*, 55–64.

(5) Kemp, D. S. *Trends Biotechnol.* **1990**, *8*, 249–255.

(6) Lewis, P. N.; Momany, F. A.; Scheraga, H. A. *Biochim. Biophys. Acta* **1973**, *303*, 211–229.

(7) Crawford, J. L.; Lipscomb, W. N.; Schellman, C. G. *Proc. Natl. Acad. Sci. U.S.A.* **1973**, *70*, 538–542.

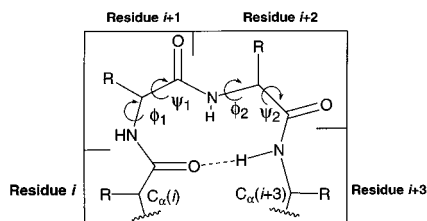


**Figure 1.** The structure of a  $\beta$ -turn.

**Table 1.** Torsion Angles for Classical  $\beta$ -Turns

torsion angle	turn type					
	I	I'	II	II'	III	III'
$\phi_1$	-60	60	-60	60	-60	60
$\psi_1$	-30	30	120	120	-30	30
$\phi_2$	-90	90	80	80	-60	60
$\psi_2$	0	0	0	0	-30	30
% occurrence	42	3	15	5	18	3

The most widely accepted system for the classification of  $\beta$ -turns is based upon the  $\phi$  and  $\psi$  peptide backbone torsion angles of residues  $i+1$  and  $i+2$  (Figure 1). The ideal torsion angles predicted by Venkatachalam are given in Table 1, although these are rarely realized in the  $\beta$ -turns actually observed in proteins.<sup>8</sup> A stringent criteria for assigning an observed  $\beta$ -turn to a given class has been set, allowing three of the four torsion angles to deviate less than  $30^\circ$  from the ideal and one angle to deviate less than  $45^\circ$ .<sup>6</sup> The type I  $\beta$ -turn is by far the most common, followed by type III and type II. The mirror image of these turns are also possible, denoted in Table 1 with a prime, although they occur far less frequently.<sup>9-11</sup>

The  $\beta$ -turn is found in all proteins, comprising approximately 25% of the amino acid residues in most proteins.<sup>1,2</sup> The location of  $\beta$ -turns at the surface of proteins and the predominance of amino acids with reactive side chains suggest they may act as key recognition elements for initiation of biological events.<sup>2</sup> The prevalence of this structural motif in small peptide ligands as well as in proteins has led to numerous efforts toward the development of analogues designed to stabilize a peptide chain in a  $\beta$ -turn conformation.<sup>4</sup> Examples of cyclic and bicyclic modifications which stabilize  $\beta$ -turns include dipeptide lactams,<sup>12-14</sup> spiroactam-bicyclic and tricyclic proline based systems,<sup>15-18</sup> the bicyclic-turned dipeptide (BTD),<sup>19,20</sup> and a number of medium-ring heterocyclic compounds.<sup>21-26</sup> In some

- (8) Venkatachalam, C. M. *Biopolymers* **1968**, *6*, 1425-1436.  
 (9) Hutchinson, E. G.; Thornton, J. M. *Protein Sci.* **1994**, *3*, 2207-2216.  
 (10) Chou, P. Y.; Fasman, G. D. *J. Mol. Biol.* **1977**, *115*, 135-175.  
 (11) Wilmot, C. M.; Thornton, J. M. *J. Mol. Biol.* **1988**, *203*, 221-232.  
 (12) Freidinger, R. M.; Perlow, D. S.; Veber, D. F. *J. Org. Chem.* **1982**, *47*, 104-109.  
 (13) Freidinger, R. M.; Brady, S. F.; Paleveda, W. J.; Perlow, D. S.; Colton, C. D.; Whitter, W. L.; Saperstein, R.; Brady, E. J.; Cascieri, M. A.; Veber, D. F. In *Clinical Pharmacology in Psychiatry*; Dahl, Gram, Paul, and Potter, Eds.; Springer-Verlag: Berlin, 1987; pp 12-19.  
 (14) Freidinger, R. M.; Veber, D. F.; Perlow, D. S.; Brooks, J. R.; Saperstein, R. *Science* **1980**, *210*, 656-658.  
 (15) Genin, M. J.; Johnson, R. L. *J. Am. Chem. Soc.* **1992**, *114*, 8778-8783.  
 (16) Genin, M. J.; Ojala, W. H.; Gleason, W. B.; Johnson, R. L. *J. Org. Chem.* **1993**, *58*, 2334-2337.  
 (17) Hinds, M. G.; Richards, N. G. J.; Robinson, J. A. *J. Chem. Soc., Chem. Commun.* **1988**, 1447-1449.  
 (18) Hinds, M. G.; Welsh, J. H.; Brennard, D. M.; Fisher, J.; Glennie, M. J.; Richards, N. G. J.; Turner, D. L.; Robinson, J. A. *J. Med. Chem.* **1991**, *34*, 1777-1789.  
 (19) Nagai, U.; Sato, K.; Nakamura, R.; Kato, R. *Tetrahedron* **1993**, *49*, 3577-3592.  
 (20) Nagai, U.; Sato, K. *Tetrahedron Lett.* **1985**, *26*, 647-650.  
 (21) Kahn, M.; Wilke, S.; Chen, B.; Fujika, K. *J. Am. Chem. Soc.* **1988**, *110*, 1638-1639.

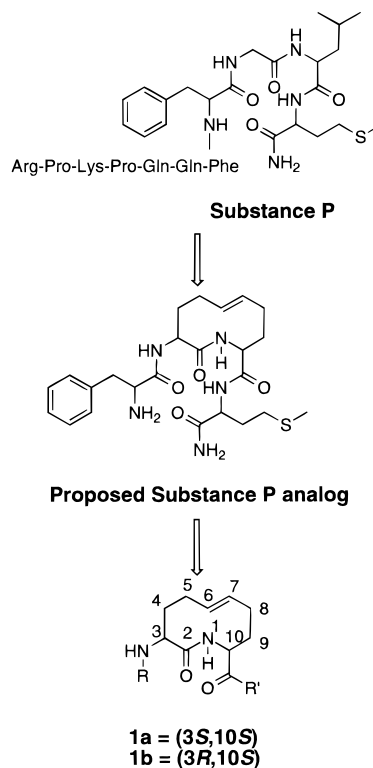


**Figure 2.** Proposed type I  $\beta$ -turn mimic (**1**) and Substance P analogue.

cases, incorporation of these structural mimics in the native peptide has led to analogues with increased biological activity or stability.<sup>14,19,27-31</sup> To date, the majority of  $\beta$ -turn mimics reported are for type II or II' turns. To our knowledge, only two examples exist of mimics for type I  $\beta$ -turns,<sup>22</sup> while these turns account for approximately 40% of the turns found in protein crystal structures. In this paper, we present our approach toward the design of a general  $\beta$ -turn mimic which is able to mimic a number of  $\beta$ -turn types, including type I  $\beta$ -turns. Additionally, the synthesis and conformational analysis of some derivatives of the mimic will be discussed.

## Results and Discussion

**Design of  $\beta$ -Turn Mimic.** Our initial interest in designing a  $\beta$ -turn mimic focused on the neuropeptide Substance P. Substance P is a biologically active undecapeptide that has been shown to play important roles in pain transmission, bronchial constriction, and vasodilation (Figure 2).<sup>32,33</sup> A  $\beta$ -turn has been observed in the final four C-terminal residues Phe<sup>8</sup>-Gly<sup>9</sup>-

- (22) Kahn, M.; Wilke, S.; Chen, B.; Fujita, K.; Lee, Y.-H.; Johnson, M. E. *J. Mol. Recog.* **1988**, *1*, 75-79.  
 (23) Kahn, M.; Nakanishi, H.; Chrusciel, R. A.; Fitzpatrick, D.; Johnson, M. E. *J. Med. Chem.* **1991**, *34*, 3395-3399.  
 (24) Olson, G. L.; Voss, M. E.; Hill, D. E.; Kahn, M.; Madison, V. S.; Cook, C. M. *J. Am. Chem. Soc.* **1990**, *112*, 323-333.  
 (25) Kemp, D. S.; McNamara, P. *Tetrahedron Lett.* **1982**, *23*, 3761-3764.  
 (26) Kemp, D. S.; Stites, W. E. *Tetrahedron Lett.* **1988**, *29*, 5057-5060.  
 (27) Ward, P.; Ewan, G. B.; Jordan, C. C.; Ireland, S. J.; Hagan, R. M.; Brown, J. R. *J. Med. Chem.* **1990**, *33*, 1848-1851.  
 (28) Sato, K.; Hotta, M.; Dong, M.-H.; Hu, H.-Y.; Taulene, J. P.; Goodman, M.; Nagai, U.; Ling, N. *Int. J. Peptide Protein Res.* **1991**, *38*, 340-345.  
 (29) Baca, M.; Alewood, P. F.; Keny, S. B. H. *Protein Struct.* **1993**, *2*, 1085-1091.  
 (30) Kahn, M.; Nakanishi, H.; Chrusciel, R. A.; Fitzpatrick, D.; Johnson, M. E. *J. Med. Chem.* **1991**, *34*, 3395-3399.  
 (31) Su, T.; Nakanishi, H.; Xue, L.; Chen, B.; Tuladhar, S.; Johnson, M. E.; Kahn, M. *Bioorg. Med. Chem. Lett.* **1993**, *3*, 835-840.  
 (32) Pagan, D. G. *Annu. Rev. Med.* **1989**, *40*, 341-352.

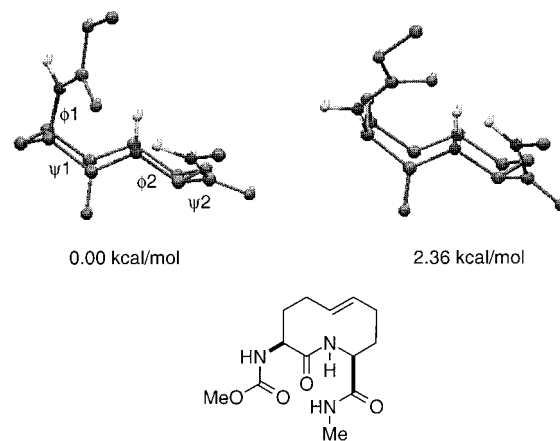
Leu<sup>10</sup>-Met<sup>11</sup> by <sup>1</sup>H NMR experiments, yet its presence has not been unambiguously established, since replacement of Gly<sup>9</sup>-Leu<sup>10</sup> with a type II or II'  $\beta$ -turn mimic did not result in a biologically active compound.<sup>13,27</sup> We envisioned that incorporation of a type I  $\beta$ -turn mimic into a substance P analogue might help to define its bioactive conformation. If Substance P adopted a type I  $\beta$ -turn, a proper analogue incorporating a type I  $\beta$ -turn mimic should show increased biological activity. We hypothesized that the Gly<sup>9</sup>-Leu<sup>10</sup> dipeptide of Substance P played structural roles and helped to orient the Phe<sup>8</sup> and Met<sup>11</sup> side chains;<sup>34</sup> hence, we elected to constrain our mimic externally in a ten-membered ring (1), through covalent attachment through the *i*+1 and *i*+2 residues (Figure 2).<sup>35</sup> While this hydrocarbon tether was designed to mimic the side chains of NK-1 selective peptides, we were more concerned with the ability of our mimic to adopt the appropriate backbone torsion angles and its potential ability to influence peptide chain direction and conformation.

**Molecular Modeling of the  $\beta$ -Turn Mimic Core.** Molecular modeling techniques were used to investigate the low energy conformations of two diastereomers of the proposed  $\beta$ -turn mimic. Monte Carlo conformational searching<sup>36</sup> and energy minimization of the 2-azacyclodec-6-enone ring systems **1a** and **1b**, where R = CO<sub>2</sub>Me and R' = NHMe, were performed using the MM2<sup>37</sup> force-field in Macromodel v. 5.5 (see Experimental Section).<sup>38</sup> The two lowest energy structures calculated for the (3*S*,10*S*) diastereomer **1a** are shown in Table 2. As predicted, the expected chair-chair conformation is the lowest in energy, whereas the second lowest energy conformation is a chair-boat. Analysis of the  $\phi$  and  $\psi$  torsion angles for the chair-chair conformation and comparison to the  $\phi$  and  $\psi$  torsion angles for an ideal type I  $\beta$ -turn indicate that in this conformation, **1a** would be a good type I  $\beta$ -turn mimic (Table 2).

A similar analysis of the (3*S*,10*R*) diastereomer **1b** shows that the lowest energy conformation (C1, Table 3) is a chair-boat and does not mimic a known type of  $\beta$ -turn. The expected chair-chair was found to be the fourth lowest in energy (C4). However, the second lowest energy (C2), at 0.98 kcal/mol, does accurately mimic a type III turn, and the third lowest in energy (C3) mimics a type II turn, within the criteria set by Lewis.<sup>6</sup> As the three lowest energy conformations are separated by less than 2 kcal/mol, the (3*S*,10*R*) diastereomer seems to be more flexible than the (3*S*,10*S*) diastereomer and should be able to access either a type II conformation or type III  $\beta$ -turn turn conformation depending on the environment at a receptor.

From these initial modeling experiments, it appeared that the (6*E*)-2-azacyclodec-6-enone ring system would be able to constrain a tetrapeptide sequence to the torsion angles found in

**Table 2.** Low Energy Conformers of (3*S*,10*S*)- $\beta$ -Turn Mimic **1a**

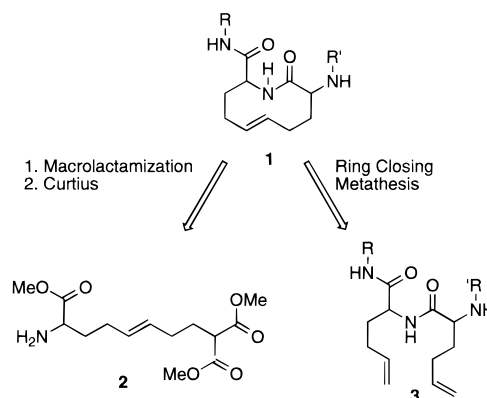


conf	rel energy (kcal/mol)	$\phi_1$ (deg)	$\psi_1$ (deg)	$\phi_2$ (deg)	$\psi_2$ (deg)
type I					
chair-chair	0.0	-60	-30	-90	0
chair-boat	2.04	-59	-24	-101	11

**Table 3.** Low Energy Conformers of (3*S*,10*R*)- $\beta$ -Turn Mimic **1b**

conf	rel energy (kcal/mol)	$\phi_1$ (deg)	$\psi_1$ (deg)	$\phi_2$ (deg)	$\psi_2$ (deg)
type II					
C1	0.0	-60	120	80	0
C2	0.98	-60	-30	-60	-30
C3	1.47	-80	-14	-65	-30
C4	2.15	-55	-26	-67	-22
		53	-82	-73	-28
		-72	128	106	-20

### Scheme 1



the three most common classes of  $\beta$ -turn. Thus, this would be useful not only as a potential Substance P mimic but also as a standard scaffold to probe the bioactive conformation of other biologically active peptides where  $\beta$ -turn structures are thought to be important.

**Synthetic Approaches.** A number of routes were explored toward the synthesis of the 2-azacyclodec-6-enone core **1** (Scheme 1), including the macrolactamization of an  $\omega$ -amino acid derivative **2** followed by Curtius rearrangement to introduce the C3 amino group and ring closing olefin metathesis of a dipeptide diolefin **3**.

**Macrolactamization Route.** The most straightforward method for the construction of the core **1** seemed to be macrolactamization. However, the number of reported syntheses of medium-sized ring (8–12-membered) lactams is few,<sup>39–41</sup> compared to the extensive literature on the preparation of small ring (3–7-

(33) Logan, M. E.; Goswami, R.; Tomczuk, B. E.; Venepalli, B. R. *Ann. Reports Med. Chem.* **1991**, *26*, 43.

(34) Srinivasan, R. Ph.D. Thesis, University of Illinois, Urbana, 1994.

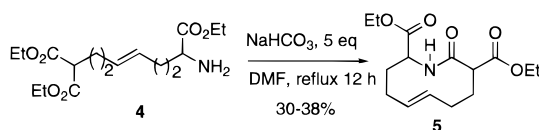
(35) Although designed independently, our proposed turn mimic bears considerable resemblance to the type II'  $\beta$ -turn mimic proposed by Kemp. However, conformational analysis and attempts at incorporation of Kemp's mimic into biologically active peptides were unsuccessful due to lack of crystallinity and problems with poor solubility and tendency towards gel formation. Kemp concluded that these problems were due to the two macrocyclic amide functionalities, which were oriented perpendicular to the plane of the turn and probably facilitated  $\beta$ -sheet formation through intermolecular associations. Our proposed mimic should alleviate these problems through replacement of one amide functionality with a surrogate trans-olefin. Kemp, D. S.; Stites, W. E. *Tetrahedron Lett.* **1988**, *29*, 5057–5060.

(36) Goodman, J. M.; Still, W. C. *J. Comput. Chem.* **1991**, *12*, 1110–1117.

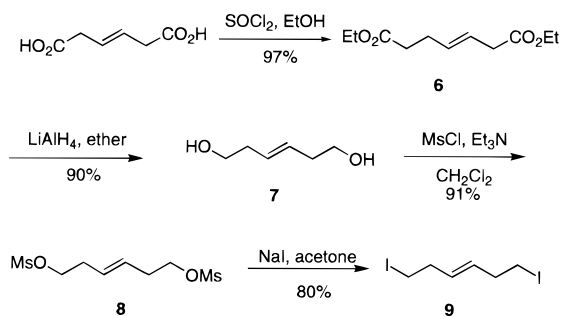
(37) Allinger, N. L. *J. Am. Chem. Soc.* **1977**, *99*, 8127–8134.

(38) Mohamadi, F.; Richards, N. G. J.; Guida, W. C.; Liskamp, R.; Lipton, M.; Caufield, C.; Chang, G.; Hendrickson, T.; Still, W. C. *J. Comput. Chem.* **1990**, *11*, 440–467.

## Scheme 2



## Scheme 3



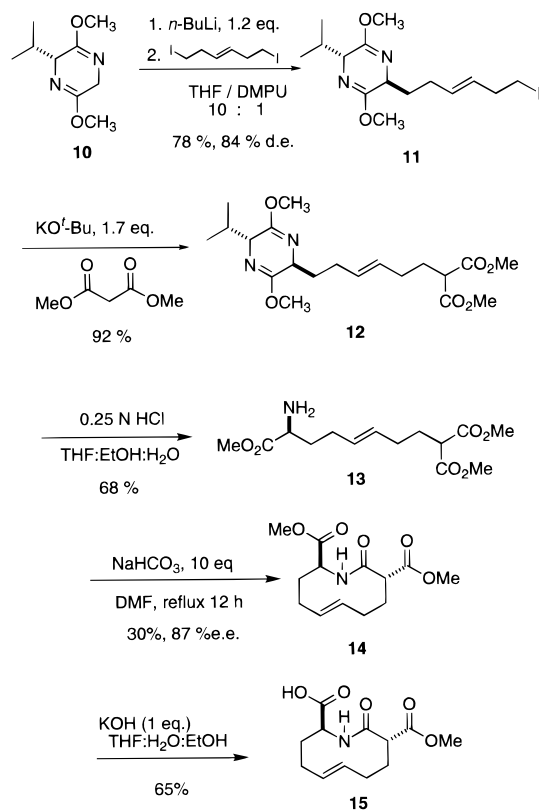
membered)<sup>42</sup> and large ring (13–30-membered) lactams.<sup>43–46</sup> The difficulty in preparing medium-sized ring lactams by cyclization of  $\omega$ -amino acids can be attributed to ring strain that develops in the transition state during formation of the medium-sized ring.<sup>47</sup>

After surveying a number of methods for the cyclization of  $\omega$ -amino acids with various activating strategies, we found that under basic conditions, refluxing aminotriester **4** in DMF at high dilution would yield a single diastereomer of **5** in modest yield (Scheme 2). Only the diastereomer in which both the C3 and C10 esters were oriented equatorially was observed, probably reflecting the higher strain energy required to force either substituent into an axial position.

The formation of a single diastereomer in the cyclization reaction encouraged us to explore an asymmetric synthesis of **5**. The stereogenic center  $\alpha$  to the amine was created by an asymmetric alkylation of Schöllkopf's chiral glycine equivalent<sup>48</sup> with a homoallylic diiodide. The preparation of the requisite unsaturated diiodide is described in Scheme 3. Commercially available *trans*- $\beta$ -hydroxyacid was refluxed in ethanol with thionyl chloride to give the diester **6** in 97% yield. Reduction of the ester with  $\text{LiAlH}_4$  afforded the diol **7**, which was subsequently mesylated with methanesulfonyl chloride and  $\text{Et}_3\text{N}$  to provide dimesylate **8**. Conversion of **8** to diiodide **9** was accomplished using a modified Finklestein reaction involving  $\text{NaI}$ .

Alkylation of Schöllkopf's auxiliary **10** with diiodide **9** proceeded with good yield and 84% de to afford iodide **11** (Scheme 4). After separation of the diastereomers by column chromatography, dimethyl malonate was alkylated with the desired (major) diastereomer **11** to afford diester **12**. Hydrolysis of the auxiliary in dilute aqueous HCl afforded the aminotriester

## Scheme 4



**13**, which was subjected to the previously described macrolactamization conditions to afford lactam **14** in moderate yield. At this point, selective hydrolysis of the C3 ester was attempted. However, treatment with  $\text{KOH}$  selectively hydrolyzed the ester at C10 to give acid **15** and gave as well a small amount of C3 epimerized **14**, both effects presumably arising through enolization at C3. Although a number of hydrolysis conditions were used, we were unable to selectively hydrolyze the C3 ester. Attempts at differentially protecting the C10 ester and then hydrolyzing the ester at C3 were also unsuccessful owing, in large part, to the insolubility of **15**. With these difficulties effectively preventing attainment of our target compound as well as the inability of this route to access the (3*S*,10*S*) diastereomer we sought a more general route to the target core structure **1**.

**Ring-Closing Olefin Metathesis Route.** As an alternative to the classic methods for the formation of lactams, cyclization through the olefin was explored. In recent years, one of the most successfully used methods for ring closure through an olefin has been ring-closing olefin metathesis (RCM).<sup>49–52</sup> In addition to its successful application to a number of ring sizes, Grubbs' ruthenium alkylidene catalysts also have a very wide range of functional group tolerance. Numerous examples are known for cyclization to form lactams, lactones, and carbocycles.<sup>53–55</sup> Yet, despite its success in the cyclization of small and large ring systems, RCM has not been used extensively to

(39) Evans, P. A.; Holmes, A. B.; Russell, K. *Tetrahedron Lett.* **1992**, 33, 6857–6858.

(40) Lease, T. G.; Shea, K. J. *J. Am. Chem. Soc.* **1993**, 115, 2248–2260.

(41) Koch, T.; Hesse, M. *Synthesis* **1992**, 931–932.

(42) Ogliastro, M. A.; Wolfe, J. F. *Synthesis of Lactones and Lactams*; John Wiley & Sons: New York, 1993.

(43) Paterson, I.; Mansuir, M. M. *Tetrahedron* **1985**, 41, 3569–3624.

(44) Corey, E. J.; Weigel, L. O.; Floyd, D.; Bock, M. G. *J. Am. Chem. Soc.* **1978**, 100, 2916–2918.

(45) Corey, E. J.; Weigel, L. O.; Chamberlin, A. R.; Cho, H.; Hua, D. H. *J. Am. Chem. Soc.* **1980**, 102, 6613–6615.

(46) Nakatsuka, M.; Ragan, J. A.; Sammakia, T.; Smith, D. B.; Uehling, D. E.; Schreiber, S. L. *J. Am. Chem. Soc.* **1990**, 112, 5583–5601.

(47) Illuminati, G.; Mandolini, L. *Acc. Chem. Res.* **1981**, 14, 95–102.

(48) Schöllkopf, U.; Neubauer, H.-J. *Synthesis* **1982**, 861–863.

(49) Nguyen, S. T.; Johnson, L. K.; Grubbs, R. H.; Ziller, J. W. *J. Am. Chem. Soc.* **1992**, 114, 3974.

(50) Nguyen, S. T.; Grubbs, R. H.; Ziller, J. W. *J. Am. Chem. Soc.* **1993**, 115, 9858–9859.

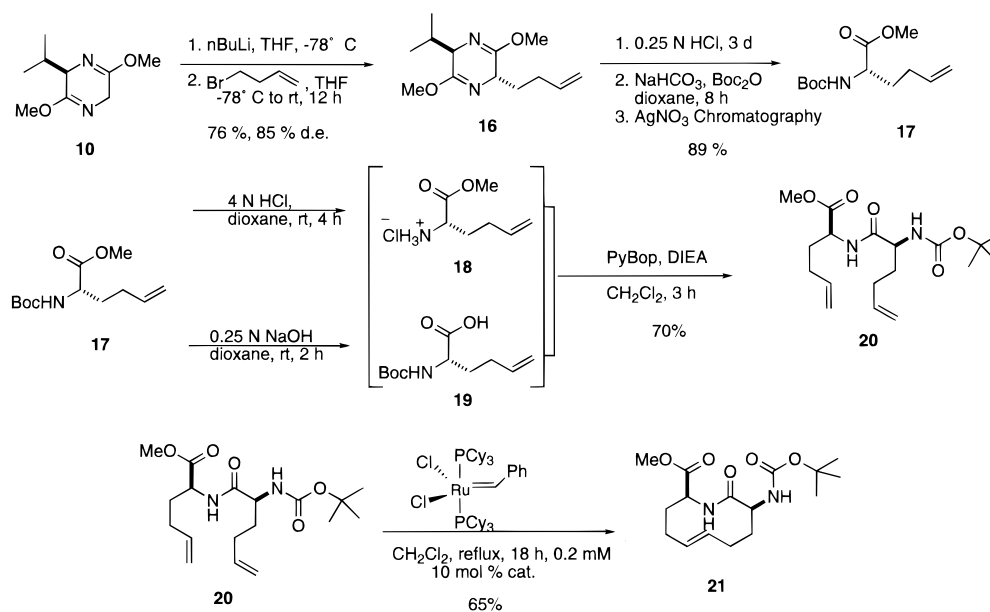
(51) Schwab, P.; Grubbs, R. H.; Ziller, J. W. *J. Am. Chem. Soc.* **1996**, 118, 100–110.

(52) Schuster, M.; Blechert, S. *Angew. Chem., Int. Ed. Engl.* **1997**, 36, 2036–2056.

(53) Grubbs, R. H.; Miller, S. J.; Fu, G. C. *Acc. Chem. Res.* **1995**, 28, 446–452.

(54) Schmalz, H. G. *Angew. Chem., Int. Ed. Engl.* **1995**, 34, 1833–1836.

## Scheme 5



form medium-sized rings.<sup>56</sup> However, we reasoned that RCM might offer advantages in the formation of medium-sized rings, because the size of ruthenium might relieve ring strain during the cyclization.<sup>57</sup>

Our synthetic approach to the core structure **1** using RCM is shown in Scheme 5. Alkylation of Schöllkopf's auxiliary **10**<sup>48</sup> with 1-bromo-3-butene afforded the alkene **16** in good yield and good diastereoselectivity. The diastereomers were readily separated by silica gel column chromatography. Hydrolysis of the auxiliary gave a mixture of the desired methyl 2-amino-5-hexenoate, along with valine methyl ester from the auxiliary. This mixture proved to be inseparable either as the free amines or the hydrochloride salts. However, upon treatment with NaHCO<sub>3</sub> and Boc<sub>2</sub>O, in a one pot procedure, the fully protected amino acid **17** was readily separable from the Boc-valine methyl ester in good yield, using argentation chromatography. Amino acid **17** was deprotected with HCl in dioxane to afford amine **18** or saponified with dilute NaOH to afford the free acid **19**. These were then coupled, without purification, using the PyBop reagent to afford the dipeptide **20** in 70% yield from **17**.

Initial attempts to carry out RCM on dipeptide **20** in benzene at ambient temperature or at reflux afforded only a mixture of dimers with low conversion. The use of methylene chloride at room temperature likewise afforded only a dimeric mixture. However, at reflux temperature and high dilution (0.8 mM), conversion of **20** to the ten-membered lactam **21** was achieved in good yield, the amount of dimer being limited to only 10–15%. *The synthesis of lactam 21 through ring closing olefin metathesis represents the first example of a ten-membered lactam cyclized using RCM. Not only does RCM allow for all of the necessary functionality of our proposed mimic but it also allows access to the (3S,10S) diastereomer that was unattainable through the macrolactamization route.* Since this diastereomer should be the most difficult to form (one substituent oriented axially), the other diastereomer (3S,10R) should be readily prepared in enantiomerically pure form, beginning from the opposite enantiomer of Schöllkopf's auxiliary. Although the success of RCM may be highly dependent on the substitution

pattern around the olefin, the high functional group tolerance and mildness of the reaction suggest the prospect of including additional reactive functionality at the *i*+1 and *i*+2 positions, contingent on the starting amino acids. Additionally, it has been demonstrated that RCM is compatible with solid-phase organic synthesis.<sup>58</sup> Since the starting monomers are simple amino acids, the wealth of methodology available for solid-phase peptide synthesis could be used to create derivatives with any peptide sequence desired. RCM, as the final step, would allow for easy incorporation of our proposed mimic into peptide probes or drug candidates.

With the core ring system in hand, tetrapeptide derivatives were prepared that would be amenable to conformational analysis and biological evaluation (Scheme 6). Removal of the Boc group with TFA and coupling to Boc-L-phenylalanine using PyBop afforded **22**. Saponification of the methyl ester in dilute NaOH was followed by PyBop coupling with L-methionamide to afford the Substance P analogue **23**. In addition to biological data, we had hoped to analyze this derivative through X-ray crystallography; however, at this time we have not successfully grown crystals of these peptide derivatives of the macrolactam that are suitable for analysis.

Compound **23** was only soluble in polar solvents (MeOH, DMSO). To conduct solution conformational analysis, derivatives that were soluble in weaker hydrogen bonding solvents were prepared (Scheme 7). Removal of the Boc-protecting group of **21** with trifluoroacetic acid, followed by PyBop coupling to Boc-L-phenylalanine or Boc-L-alanyl-L-phenylalanine provided the tripeptide **22** and tetrapeptide **24**, respectively. Saponification of the methyl ester followed by peptide coupling to L-phenylalanine methyl ester afforded the tetrapeptide **25a** and pentapeptide **25b**, respectively, in good yield.

Tetrapeptide **25a** and pentapeptide **25b** proved to be soluble in a wide variety of solvents, allowing conformational analysis in both polar and nonpolar environments. The <sup>1</sup>H NMR spectra of **25a** showed no spectral overlap, allowing complete assignment of all peptide chain resonances and determination of coupling constants. The pentapeptide **25b** was prepared in order

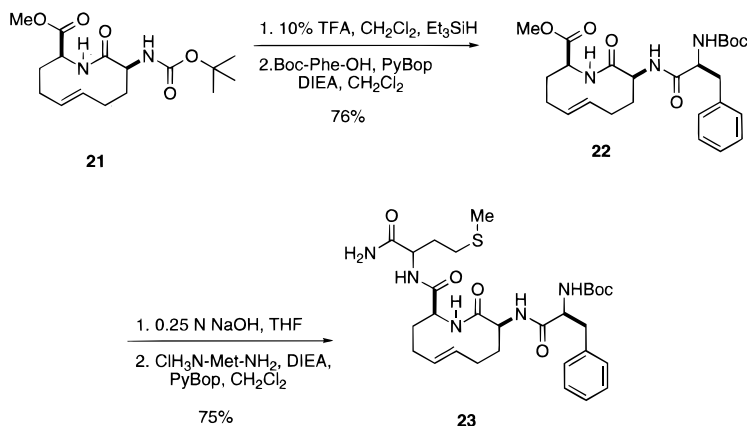
(55) Snapper, M. L.; Tallarico, J. A.; Randall, M. L. *J. Am. Chem. Soc.* **1997**, *119*, 1478–1479.

(56) Furstner, A.; Muller, T. *Synlett* **1997**, 1010–1012.

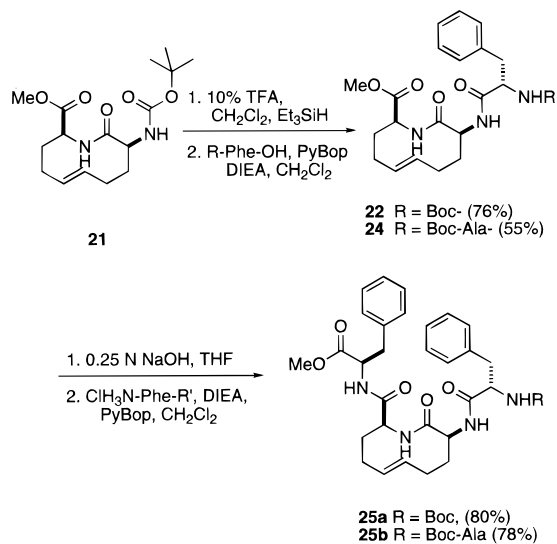
(57) Furstner, A.; Langemann, K. *Synthesis* **1997**, 792–803.

(58) Miller, S. J.; Blackwell, H. E.; Grubbs, R. H. *J. Am. Chem. Soc.* **1996**, *118*, 9606–9614.

## Scheme 6



## Scheme 7



to determine what effect an additional amino acid substituent at the C-terminus would have on molecular conformation.

**Conformational Analysis of the Macrolactam  $\beta$ -Turn Mimic and Derivatives.** There are a number of approaches for the determination of peptide conformation. Typical methods such as X-ray crystallography, NMR spectroscopy, and molecular modeling all provide insight; however, peptide conformation is strongly influenced by its environment. As such, the conformation found in solution, in the solid state, or as a theoretical minimum in a vacuum or in a simulated solvent is not necessarily the true conformation, nor the one adopted when the peptide is receptor bound. Integration of the results from all three methods of analysis, along with evaluation of biological activity, can provide the best idea of peptide conformation. Since we were unable to prepare crystals of the peptide derivatives of the macrolactam core **23** or **25** suitable for X-ray analysis, compounds **21**, **22**, and **25a** were analyzed through as many of the above-mentioned techniques as possible, to try to gain insight as to the final conformation.

The core macrolactam **21** gave crystals suitable for X-ray analysis by the slow evaporation of a methanolic solution. Two different conformations were observed in the unit cell, that of a chair-chair and that of a chair-boat, related through a ring flip at C3 (Figure 3).

This is nicely in accord with our initial modeling, as described earlier, in which we found the chair-chair and chair-boat to be the two lowest energy structures. Analysis of the torsion

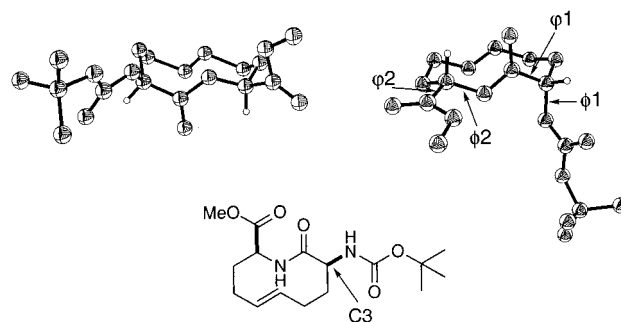


Figure 3. ORTEP diagram of (3*S*,10*S*)-**21**.

Table 4. Calculated, X-ray, and Ideal Type I  $\beta$ -Turn Torsion Angles

conf	rel energy (kcal/mol)	$\phi_1$ (deg)	$\psi_1$ (deg)	$\phi_2$ (deg)	$\psi_2$ (deg)
type I		-60	-30	-90	0
Calculated Lowest Energy Structures for <b>1a</b>					
chair-chair	0.0	-59	-24	-101	11
chair-boat	2.04	56	-80	-106	-12
X-ray Structures of <b>21</b>					
chair-chair		-107	-1	-130	23
chair-boat		120	-64	-131	-43

angles found in the X-ray structure and comparison with the angles calculated from the lowest energy structures are shown in Table 4.

Although the torsion angles were not as close as expected, the central two angles  $\psi_1$  and  $\phi_2$  are within 30° of the calculated angles. When assigning a  $\beta$ -turn to a given class, Lewis has used a criteria of less than 30° deviation from three of the standard angles and deviation of one angle by less than 45°.<sup>9</sup> When compared in this manner, the ten-membered lactam does constrict the central two angles close to those of a type I  $\beta$ -turn, although not ideally.

In solution, the <sup>1</sup>H NMR spectrum of **21** showed some signals that were unusually broad (Figure 4). Upon cooling to -30 °C, two different conformational isomers were observed, although poor resolution prevented rigorous assignment of resonances to any specific conformation. However, at 25 °C the proton at C10 (H<sup>10</sup>) shows a large coupling constant (12.1 Hz) to the axial proton at C9 (H<sup>9ax</sup>), indicating that the methyl ester was oriented equatorially, and a large coupling constant to the ring amide proton H<sup>1</sup> (10.0 Hz), indicating that the H<sup>10</sup> and H<sup>1</sup> protons are approximately 180° to one another. These data would seem to indicate a chairlike conformation for this portion of the molecule, which is in complete accord with the

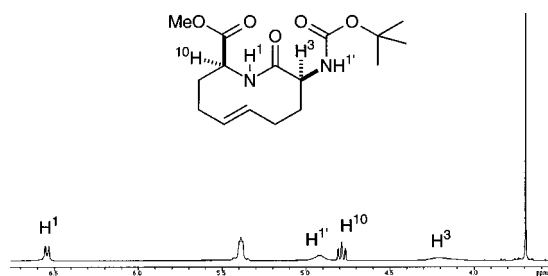
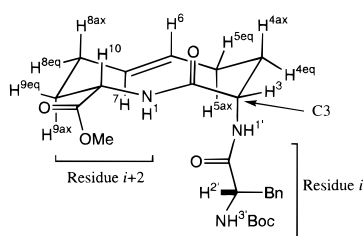


**Figure 4.**  $^1\text{H}$  NMR spectrum of **21** at 25 °C.

**Table 5.** Analysis of Vicinal Coupling Constants for Tripeptide **22**



protons	$J$ obsd, Hz	protons	$J$ obsd, Hz
$\text{H}^3\text{-H}^{4\text{ax}}$	2.90	$\text{H}^{10}\text{-H}^{9\text{ax}}$	11.90
$\text{H}^3\text{-H}^{4\text{eq}}$	4.90	$\text{H}^{10}\text{-H}^{9\text{eq}}$	2.20
$\text{H}^3\text{-H}^{1'}$	8.24	$\text{H}^{10}\text{-H}^1$	10.10

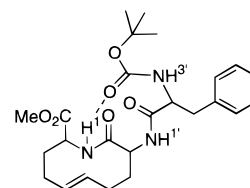
results of the X-ray analysis. The resonances for  $\text{H}^3$  and  $\text{H}^{1'}$  are broadened by relatively slow conformational averaging between a chair and boat conformation for this portion of the molecule, again in accord with the X-ray analysis.

*Conformational analysis, through X-ray crystallography and  $^1\text{H}$  NMR, has shown that **21** may adopt either a chair–chair or a chair–boat conformation, both in solution and in the solid state. In addition, these results demonstrate that the methods used for conformational analysis are self-consistent and that we observe the same dynamics by either method. While such a conformational equilibrium is undesirable in a peptidomimetic, **21** is a dipeptide without the potential intramolecular hydrogen bond donors of a tetrapeptide  $\beta$ -turn mimic. The inclusion of potential hydrogen bond donating groups at the  $i$  and  $i+3$  positions may help to stabilize a single conformation.*

The  $^1\text{H}$  NMR spectrum of compound **22** showed a single conformation at low temperature, indicating that some intramolecular hydrogen bonding was probably taking place, stabilizing one conformation. All resonances were now clearly resolved, and coupling constants were obtained that matched well with the expected chair–chair conformation. Proton  $\text{H}^{10}$  still showed a large coupling to  $\text{H}^{9\text{ax}}$  (11.9 Hz) and a large coupling to the amide proton  $\text{H}^1$  (10.1 Hz); however, now  $\text{H}^3$  is resolved and shows two small couplings (2.9 and 4.9 Hz) to vicinal neighbors, indicating the amine substituent at C3 is in an axial position (Table 5).

To establish whether any intramolecular hydrogen bonds were forming, a series of  $^1\text{H}$  NMR experiments were conducted to determine the effect of solvent, concentration, and temperature on amide proton chemical shift. In all three cases (Table 6), the amide proton of the ring ( $\text{H}^1$ ) shows a smaller chemical shift dependence on temperature, concentration, and solvent. The only possible intramolecular hydrogen bond acceptors available to this hydrogen are the carbonyl oxygen of the Boc group (forming a ten-membered ring) or the carbonyl of the  $i$  residue (forming a seven-membered ring). Since no intramolecular hydrogen bond was observed in **21**, where there is the

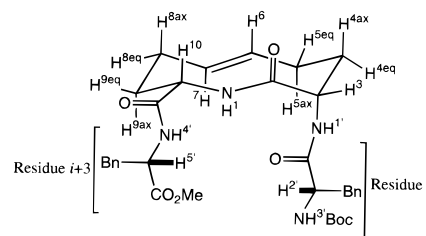
**Table 6.** Proposed Intramolecular Hydrogen-Bonding Pattern for Tripeptide **22**



proton	$\Delta\delta/\Delta T$ ( $\text{CD}_3\text{CN}$ ) <sup>a</sup> $10^3$ ppm/K	$\Delta\delta/\Delta C$ ( $\text{CDCl}_3$ ) <sup>b</sup> ppm/M	$\Delta\delta/\Delta\text{solvent}$ ( $\text{CD}_3\text{CN}-\text{CDCl}_3$ ) ppm/solvent
$\text{H}^1$	1.5	0.15	0.03
$\text{H}^{1'}$	2.1	0.85	0.22
$\text{H}^{3'}$	4.5	1.23	0.60

<sup>a</sup>  $\Delta T = 25\text{--}60$  °C, 0.028 M, 500 MHz. <sup>b</sup>  $\Delta C = 0.25\text{--}0.001$  M, 25 °C, 500 MHz.

**Table 7.** Analysis of Intramolecular Hydrogen-Bonding Pattern for Tetrapeptide **25a**



proton	$\Delta\delta/\Delta T$ ( $\text{CD}_3\text{CN}$ ) <sup>a</sup> $10^3$ ppm/K	$\Delta\delta/\Delta C$ ( $\text{CDCl}_3$ ) <sup>b</sup> ppm/M	$\Delta\delta/\Delta\text{solvent}$ ( $\text{CD}_3\text{CN}-\text{CDCl}_3$ ) ppm/solvent
$\text{H}^1$	1.6	0.07	0.00
$\text{H}^{1'}$	3.2	0.25	0.17
$\text{H}^{3'}$	3.8	0.40	0.72
$\text{H}^{4'}$	2.5	0.17	0.28

<sup>a</sup>  $\Delta T = 25\text{--}65$  °C, 0.031 M, 500 MHz. <sup>b</sup>  $\Delta C = (0.25\text{--}0.001)$  M, 25 °C, 500 MHz.

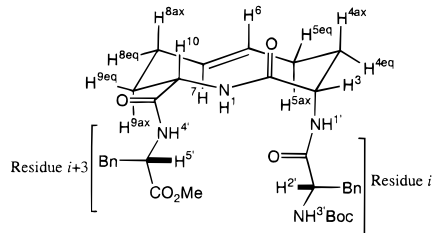
possibility for the formation of the same seven-membered ring, it is likely that the carbonyl of the Boc group forms a ten-membered ring as shown in Table 6.

It is well-known that type I  $\beta$ -turns show a preference for amino acids in the  $i$  position that have strongly hydrogen bond accepting side chains (Asn, Asp, Cys, Ser).<sup>9</sup> These residues stabilize the turn by forming an intramolecular hydrogen bond with the main-chain nitrogen of the third residue, creating a ten-membered ring. In these cases, the side chain and main chain of residue  $i$ , along with the  $i+1$  and  $i+2$  residues, form another turn type structure.<sup>9,59</sup> A similar turn may be formed between the carbonyl oxygen of the Boc-protecting group and the amide proton  $\text{H}^1$  of the ten-membered lactam.

*These results were encouraging, since they indicate that **22** seems to mimic the behavior of naturally occurring type I  $\beta$ -turns. This intramolecular hydrogen bond probably slows the ring flip that led to broadening of the  $^1\text{H}$  NMR resonances for  $\text{H}^3$  and  $\text{H}^{1'}$  in compound **21** and stabilizes a single conformation for **22**. Through analysis of coupling constants, we are now able to assign a chair–chair conformation to the ten-membered lactam portion of **22**.*

A similar analysis of potential hydrogen bonding patterns for tetrapeptide **25a** was conducted, and the results are shown in Table 7. Again, the chemical shift for  $\text{H}^1$  shows the smallest dependence on concentration, temperature, and solvent. This

(59) Rees, D. C.; Lewis, M.; Lipscomb, W. N. *J. Mol. Biol.* **1983**, *168*, 367–387.

**Table 8.** Observed Coupling Constants and Calculated Dihedral Angles


protons	$J$ obsd, Hz	calcd dihedral angles	protons	$J$ obsd, Hz	calcd dihedral angles
H <sup>3</sup> -H <sup>4ax</sup>	2.93	49.10	H <sup>10</sup> -H <sup>9ax</sup>	11.53	177.06
H <sup>3</sup> -H <sup>4eq</sup>	5.12	-65.90	H <sup>10</sup> -H <sup>9eq</sup>	1.83	-70.90
H <sup>3</sup> -H <sup>1'</sup>	6.59	-138.19	H <sup>9ax</sup> -H <sup>8ax</sup>	14.89	
H <sup>4ax</sup> -H <sup>5ax</sup>	13.80		H <sup>9ax</sup> -H <sup>8eq</sup>	2.93	
H <sup>4ax</sup> -H <sup>5eq</sup>	3.42		H <sup>10</sup> -H <sup>1</sup>	9.10	-166.57

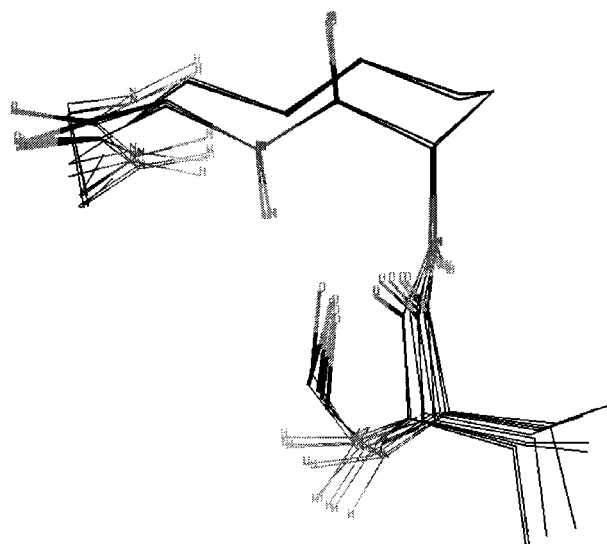
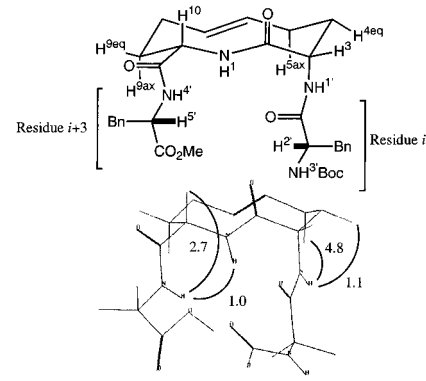
indicates that the hydrogen bond formed between the Boc carbonyl oxygen and the ring amide proton is not disrupted by the addition of the  $i+3$  residue. Although the existence of an intramolecular hydrogen bond between the carbonyl of the  $i$  residue and the NH of the  $i+3$  residue is a good indication of the formation of a  $\beta$ -turn, it is not necessary; many examples of "open" turns exist.

Analysis of vicinal coupling constants for **25a** along the peptide backbone indicated that the ten-membered lactam remained in the expected chair-chair conformation (Table 8). The protons at H<sup>3</sup> showed small couplings to protons at H<sup>4</sup>, indicating it was oriented in an equatorial manner, while the proton H<sup>10</sup> showed one large coupling (11.53 Hz) to the axial proton H<sup>9ax</sup> and one small coupling (1.83 Hz) to the equatorial proton H<sup>9eq</sup>. The remaining coupling constants around the ring support a chair-chair conformation with typical gauche interactions. Using the modified Karplus equations of Pardi,<sup>60</sup> which relates peptide dihedral angles to coupling constants, we calculated dihedral angles from the vicinal coupling constants of the ring and from the two  $J_{N\alpha}$  coupling constants (Table 8). These dihedral angles were used as torsional constraints for molecular modeling on the tetrapeptide mimic (see Experimental Section).

The 10 lowest energy structures (within 1 kcal/mol of the global minimum) are overlaid in Figure 5. It is immediately apparent that a hydrogen bond is formed between the Boc carbonyl oxygen and ring amide proton in the 10 lowest energy structures. This is supported by the above <sup>1</sup>H NMR data. The calculated distance between this carbonyl oxygen and the nitrogen of the ten-membered lactam is 2.5 Å. Equally apparent is that the 10 lowest energy structures differ very little in the torsional bonds constrained by the ten-membered ring. Minor differences in energy arise from slight twists of the  $\psi_2$  angle and rotations around the benzyl side chains of the  $i$  and  $i+3$  phenylalanine residues (not shown).

Although vicinal coupling constants allow the determination of dihedral angles and the geometry about a given residue, they offer little information about the overall conformation of our mimic, i.e., between residues. To investigate the relative orientation between residues and possibly lend support to our model, NOE experiments were conducted. The results of 1-D NOE experiments are shown in Table 9.

A number of informative interresidue NOEs are observed. Of particular interest is the very strong NOE between H<sup>1'</sup> and

**Figure 5.** Ten lowest energy structures calculated using Monte Carlo-molecular mechanics and torsional restrictions derived from vicinal coupling constants. The phenylalanine side chains and Boc-group have been removed for clarity.**Table 9.** Interresidue NOEs for Compound **25a**


proton pair	percent NOE	calcd distance (Å)	proton pair	percent NOE	calcd distance (Å)
H <sup>1'</sup> -H <sup>5ax</sup>	4.75	2.1	H <sup>4'</sup> -H <sup>10</sup>	2.66	3.0
H <sup>4'</sup> -H <sup>1</sup>	1.02	2.2	H <sup>1'</sup> -H <sup>4eq</sup>	1.12	2.9

Numbers represent percent NOE. Phenylalanine sidechains and tbutyl groups removed.

the axial proton H<sup>5ax</sup>. This result indicates that H<sup>1'</sup> is oriented beneath the ten-membered ring, closer to H<sup>5ax</sup> than to H<sup>4eq</sup>. This is strong support for our model in which the distance between H<sup>1'</sup> and H<sup>5ax</sup> is 2.1 Å and the distance between H<sup>1'</sup> and H<sup>4eq</sup> is 2.8 Å. Assuming a *trans*-amide at the  $i$  residue, these NOEs define the  $\phi_1$  torsion angle. At the  $i+3$  position, an NOE between H<sup>4'</sup> and H<sup>1</sup>, and between H<sup>4'</sup> and H<sup>10</sup>, but not between H<sup>4'</sup> and H<sup>9eq</sup>, indicates the NH of the  $i+3$  residue is oriented toward the interior of the pseudo-ten-membered ring and above the plane of the turn. Again, this is seen in the calculated model in which both H<sup>1</sup>, H<sup>10</sup>, and H<sup>4'</sup> are within 3 Å of one another, but H<sup>9eq</sup> is 4 Å from H<sup>4'</sup>.

Thus, the experimental <sup>1</sup>H NMR data, both in terms of coupling constants and interresidue NOEs, support the calculated model. The torsion angles calculated from this model are shown in Table 10, along with comparisons to an ideal type I turn and our initial design modeling. Although there are differences between the torsion angles initially calculated and

(60) Pardi, A.; Billeter, M.; Wuthrich, K. *J. Mol. Biol.* **1984**, *180*, 741-751.



**Table 10.** Comparison of Ideal Type I  $\beta$ -Turn, **1a**, and **25a**

conf	$\phi_1$ (deg)	$\psi_1$ (deg)	$\phi_2$ (deg)	$\psi_2$ (deg)
ideal type I	-60	-30	-90	0
initial model <b>1a</b>	-59	-24	-101	11
<b>25a</b>	-82	-20	-107	-18

**Table 11.** Comparison of Vicinal Coupling Constants for **23** and **25a,b**

compd (solvent)	${}^3J_{N\alpha}$ , ${}^3J_{\alpha\beta^1}$ , ${}^3J_{\alpha\beta^2}$ (Hz)	
	H <sup>3</sup>	H <sup>10</sup>
<b>23</b> (DMF)	7.57, 4.64, 3.17	9.69, 11.23, 1.76
<b>25a</b> (CD <sub>2</sub> Cl <sub>2</sub> )	6.60, 5.12, 2.93	9.10, 11.53, 1.83
<b>25b</b> (CD <sub>2</sub> Cl <sub>2</sub> )	6.90, 4.70, 3.10	9.50, 11.70, 2.10

those determined from modeling using a number of experimental constraints, the differences are small, less than 30°.

Analysis of the coupling constants for the ring  $\alpha$ -protons and hydrogen bonding patterns for the tetrapeptide **23** and pentapeptide **25b** shows no significant differences from those of **25a** in different solvents varying in polarity (Table 11). That all derivatives maintain a similar conformation under a variety of conditions lends support for the effectiveness of the 2-azacyclodec-6-enone ring system **1** to stabilize a turn conformation.

## Conclusions

In this study we have presented a rational design of a  $\beta$ -turn mimic (**1**) capable of restricting the  $\phi$  and  $\psi$  torsion angles of a tetrapeptide to those found in type I  $\beta$ -turns. *Ring-closing olefin metathesis was shown to be an effective method for closing a medium-ring lactam under mild conditions with good yields, representing the first example of cyclization to form a ten-membered lactam using RCM.* We anticipate that RCM will greatly facilitate the synthesis of previously difficult-to-cyclize medium-ring macrocycles. A combination of NMR experiments, X-ray crystallography and molecular modeling was used to analyze the conformation of a series of derivatives of **1**. *The results of this analysis showed that the tetrapeptide derivative 25a restricted the central  $\phi$  and  $\psi$  torsion angles to within 30° of the ideal angles for a type I  $\beta$ -turn. This is, to our knowledge, only the third example of a type I  $\beta$ -turn mimic reported in the literature and the first to allow for versatile incorporation into biological systems.* We believe that this system may serve as a useful conformational constraint when incorporated into other biologically significant peptides where a  $\beta$ -turn is thought to be important.<sup>61</sup>

## Experimental Section

**General Procedures.** Reaction progress was monitored by analytical thin-layer chromatography (TLC), using 0.25 mm silica gel glass-backed plates with a UV sensitive indicator. Flash chromatography was performed using 32–63  $\mu$ m silica gel packing unless otherwise noted. Visualization was accomplished by potassium permanganate spray reagent, iodine vapors, or UV illumination (254 nm). <sup>1</sup>H NMR and <sup>13</sup>C NMR spectra were recorded at 400, 500, or 750 MHz. HMBC and HMQC spectra were recorded at 500 MHz. Chemical shifts ( $\delta$ ) are reported as parts per million from an internal tetramethylsilane (TMS) standard in the solvent indicated at 25 °C unless otherwise noted. Coupling constants were determined from <sup>1</sup>H NMR, {<sup>1</sup>H}<sup>13</sup>C decoupled NMR, or through phase-sensitive DQF NMR spectroscopy. High-pressure liquid chromatography (HPLC) was performed using ultraviolet detection at 254 nm. For analytical purposes a 4 mm  $\times$  32 cm C-18 column was used with the solvent system indicated. Elemental analysis was performed by the Microanalytical Service Laboratory at the University of Illinois.

All reactions using water- or air-sensitive reagents were conducted under an Ar atmosphere with dry solvents. Solvents were distilled under N<sub>2</sub> as follows: CH<sub>2</sub>Cl<sub>2</sub> from CaH<sub>2</sub>, THF from sodium benzophenone ketyl, DMF from MgSO<sub>4</sub>, and hexanes from CaSO<sub>4</sub>. The following reagents were purchased from commercial sources and purified before use as follows: triethylamine and diisopropylamine distilled from CaH<sub>2</sub>, 1-bromo-3-butene fractionally distilled, and dimethyl malonate fractionally distilled. All other reagents were purchased from commercial suppliers and used without further purification.

**Molecular Modeling.** Conformational searches and energy minimizations were performed using Macromodel version 5.5.<sup>38</sup> The Macromodel implementation of either the AMBER<sup>62</sup> all-atom force field or MM2 were used (respectively denoted AMBER\* and MM2\*). All calculations were performed using the implicit water or CHCl<sub>3</sub> GB/SA solvation model of Still et al.<sup>63</sup> Only small differences were noted between force-fields used or between solvation models. The data reported in this paper is using MM2\* with a water solvation. Conformational searches were performed using the Monte Carlo method of Goodman and Still.<sup>36</sup> All amide bonds and olefins were required to be trans, those deviating more than 90° being rejected as energetically improbable. For each search, 10 000 starting structures were generated and minimized to an energy convergence of 0.001 (kcal/mol)/Å using the truncated Newton–Raphson method implemented in Macromodel. Duplicate structures and those greater than 20 kcal/mol above the global minimum were discarded. In modeling the tetrapeptide **25a**, the dihedral angles constraints found in Table 8 were used with the FXTA command in Batchmin version 5.5 with a force constant of 9999.0 kcal/mol.

**(2R)-2-(3-Butenyl)-5-isopropyl-3,6-dimethoxy-2,5-dihydropyrazine (16).** To a solution of Schöllkopf's auxiliary **10** (2.0 g, 10.9 mmol) in THF (50 mL) at -78 °C was added a 1.15 M solution of *n*BuLi (12.3 mL, 14.1 mmol) in hexanes. The amber solution was allowed to stir at -78 °C for 1 h. A solution of 1-bromo-3-butene (4.4 mL, 43.6 mmol) in THF (20 mL) was slowly added via syringe to the above anion. The reaction mixture was allowed to stir for 12 h at -78 °C and then warmed to room temperature for 2 h. Water (10 mL) was added, and the reaction mixture was concentrated to a viscous oil. The residue was extracted 6  $\times$  10 mL with ether. The pooled organic extracts were dried over MgSO<sub>4</sub>, filtered, and concentrated to a yellow oil. Flash chromatography (7% ether/hexanes) afforded **16** as a clear oil (2.07 g, 80%). *R<sub>f</sub>*: 0.33 (7% ether/hexanes); [ $\alpha$ ]<sub>D</sub><sup>25</sup> +7.89 (*c* = 1, CHCl<sub>3</sub>); IR (film)  $\nu$  2958.4, 2945.7, 2930.7, 1702.8, 1697.7, 1692.5, 1687.6, 1681.7; <sup>1</sup>H NMR (CDCl<sub>3</sub>, 500 MHz)  $\delta$  5.80 (ddt, 1H, *J* = 17.0, 10.3, 6.6 Hz), 5.02 (ddt, 1H, *J* = 17.2, 2.2, 1.5 Hz), 4.93 (ddt, 1H, *J* = 10.3, 2.5, 1.3 Hz), 4.0 (dt, 1H, *J* = 6.4, 4.0 Hz), 3.91 (t, 1H, *J* = 3.5 Hz), 3.67 (s, 3H), 3.66 (s, 3H), 2.24 (sept d, 1H, *J* = 6.7, 3.3 Hz), 2.04 (m, 2H), 1.90 (dddd, 1H, *J* = 14.1, 9.5, 6.4, 4.2 Hz), 1.76 (dddd, 1H, *J* = 13.2, 10.1, 6.6, 5.3 Hz), 1.02 (d, 3H, *J* = 7.0 Hz), 0.67 (d, 3H, *J* = 6.8 Hz); <sup>13</sup>C NMR (CDCl<sub>3</sub>, 100 MHz) 163.8, 163.6, 138.5, 114.5, 60.8, 54.9, 52.3, 33.4, 31.7, 28.9, 19.0, 16.6; MS (EI, 70 eV) *m/z* (relative intensity, %) 238.1(11), 223.1 (41), 195.1 (100). Anal. Calcd for C<sub>13</sub>H<sub>22</sub>N<sub>2</sub>O<sub>2</sub>: C, 65.52; H, 9.30; N, 11.7. Found: C, 65.25; H, 9.32; N, 11.83.

**Minor diastereomer R<sub>f</sub>**: 0.28 (7% ether/hexanes); [ $\alpha$ ]<sub>D</sub><sup>25</sup> -83.13 (*c* = 1, CHCl<sub>3</sub>); <sup>1</sup>H NMR (CDCl<sub>3</sub>, 500 MHz)  $\delta$  5.84 (ddt, 1H, *J* = 17.0, 10.4, 6.6 Hz), 5.03 (dq, 1H, *J* = 17.0, 1.7 Hz), 4.95 (ddt, 1H, *J* = 10.3, 2.2, 1.1 Hz), 3.97 (dt, 1H, *J* = 8.6, 4.8 Hz), 3.91 (dd, 1H, *J* = 4.8, 3.8 Hz), 3.66 (s, 3H), 3.65 (s, 3H), 2.20 (m, 3H), 1.96 (dddd, 1H, *J* = 14.1, 10.1, 6.4, 4.4 Hz), 1.55 (m, 1H), 1.04 (d, 3H, *J* = 6.8 Hz), 0.71 (d, 3H, *J* = 6.8 Hz); <sup>13</sup>C NMR (CDCl<sub>3</sub>, 100 MHz) 163.71, 163.02, 60.83, 55.08, 52.18, 34.77, 31.21, 30.21, 19.51, 17.40.

**Methyl (2R)-2-(tert-Butoxycarbonylamino)-5-hexenoate (17).** To bis-lactim ether **16** (2.0 g, 8.40 mmol) at room temperature was added

(61) Compound **23** was tested for biological activity in a competitive inhibition assay versus radiolabeled Substance P. Tetrapeptides **23** showed no activity, which may mean that Substance P adopts a different conformation at the receptor than that adopted by our proposed mimic.

(62) Weiner, S. J.; Kollman, P. A.; Case, D. A.; Singh, U. C.; Ghio, C.; Alagona, G.; Profeta, S.; Weiner, P. *J. Am. Chem. Soc.* **1984**, *106*, 765–784.

(63) Still, W. C.; Tempczyk, A.; Hawely, R. C.; Hendrickson, T. *J. Am. Chem. Soc.* **1990**, *112*, 6127–6129.

0.25 N HCl (84 mL, 21 mmol). The suspension was allowed to stir at room temperature for 3 days. Solid NaHCO<sub>3</sub> (3.53 g, 42 mmol) was added in two equal portions at 0 °C. Dioxane (80 mL) was added followed by Boc<sub>2</sub>O (2.2 g, 10.08 mmol) at 0 °C. Reaction mixture was allowed to stir for 18 h. Dioxane was removed under reduced pressure, and residue was extracted 10 × 20 mL with EtOAc. Organic extracts were pooled, dried over Na<sub>2</sub>SO<sub>4</sub>, filtered, and concentrated to a clear/colorless oil. Flash chromatography on 15% AgNO<sub>3</sub> impregnated silica gel (15% ether/hexanes) afforded **17** as a colorless oil (1.4 g, 70%). *R*<sub>f</sub>: 0.30 (20% ether/hexanes); [ $\alpha$ ]<sub>D</sub><sup>25</sup> -22.4 (*c* = 1, MeOH); lit.<sup>61</sup> [ $\alpha$ ]<sub>D</sub><sup>25</sup> -17 (*c* = 1.2, MeOH); <sup>1</sup>H NMR (CDCl<sub>3</sub>, 500 MHz)  $\delta$  5.85 (ddt, 1H, *J* = 17.1, 10.3, 6.6 Hz), 5.10 (dq, 1H, *J* = 17.1, 3.2, 1.5 Hz), 5.08 (bs, 1H), 5.04 (dq, 1H, *J* = 10.3, 2.8, 1.2 Hz), 2.14 (q, 2H, *J* = 7.3 Hz), 1.92 (dtd, 1H, *J* = 13.7, 8.1, 5.1 Hz), 1.73 (dtd, 1H, *J* = 13.4, 8.3, 6.6 Hz), 1.42 (s, 9H); <sup>13</sup>C NMR (CDCl<sub>3</sub>, 100 MHz) 173.33, 155.33, 136.96, 115.68, 79.86, 52.95, 52.23, 31.95, 29.345, 28.28; MS (EI, 70 eV) *m/z* (relative intensity) 238.1 (M<sup>+</sup>, 20), 223 (25), 207 (14), 195 (100), 181 (15), 166 (25); Anal. Calcd for C<sub>12</sub>H<sub>21</sub>NO<sub>4</sub>: C, 58.59; H, 8.73; N, 5.69. Found: C, 58.65; H, 8.92; N, 5.63.

**Methyl 2-((*tert*-Butoxycarbonylamino)-5-hexenoyl)amino)-5-hexenoate (20).** To a solution of **17** (470 mg, 1.90 mmol) in THF (10 mL) at 0 °C was added a 0.25 N solution of NaOH (23 mL, 5.80 mmol). The reaction mixture was warmed to room temperature and stirred for 6 h. After neutralizing with 0.50 N HCl, the reaction mixture was extracted 5 × 10 mL with EtOAc. The organic extracts were dried over Na<sub>2</sub>SO<sub>4</sub>, filtered, and concentrated to a yellow oil. In a separate flask was placed **17** (470 mg, 1.90 mmol) and dioxane (5 mL). The flask was cooled to 0 °C and Et<sub>3</sub>SiH (0.3 mL, 1.9 mmol) was added. To this clear solution was added 4 N HCl in dioxane (3 mL). The reaction mixture was warmed to room temperature for 2 h and concentrated to a white solid. After drying both the free acid and amine salt under vacuum for 24 h, they were combined and dissolved in CH<sub>2</sub>Cl<sub>2</sub> (10 mL). DIEA (0.99 mL, 5.7 mmol) was added, followed by PyBop. The reaction was allowed to stir for 9 h and then concentrated to an orange oil. The residue was taken up in EtOAc and washed consecutively with 5% KHSO<sub>4</sub> (10 mL), 5% NaHCO<sub>3</sub> (10 mL), brine (10 mL), and dried over Na<sub>2</sub>SO<sub>4</sub>. After filtering and concentrating to an orange oil, flash chromatography (25% EtOAc/hexanes) afforded **20** as a white solid (476 mg, 71%). *R*<sub>f</sub>: 0.32 (25% EtOAc/hexanes); mp: 131–132 °C (EtOAc/hexanes); [ $\alpha$ ]<sub>D</sub><sup>25</sup> -5.84 (*c* = 1.15, CHCl<sub>3</sub>); <sup>1</sup>H NMR (CDCl<sub>3</sub>, 500 MHz)  $\delta$  6.60 (d, 1H, 8.1 Hz), 5.17 (d, 1H, *J* = 7.4 Hz), 5.01 (dt, 2H, *J* = 17.4, 3.2, 1.7 Hz), 4.96 (ddq, 2H, *J* = 10.1, 5.3, 3.1, 1.1 Hz), 4.59 (dt, 1H, *J* = 7.9, 4.9 Hz), 4.09 (q, 1H, *J* = 7.2), 3.72 (s, 3H), 2.08 (m, 4H), 1.93 (ddt, 1H, *J* = 13.4, 8.2, 5.1 Hz), 1.85 (m, 1H), 1.76 (dtd, 1H, *J* = 13.9, 7.9, 6.2 Hz), 1.69 (dq, 1H, *J* = 15.4, 7.7 Hz), 1.42 (s, 9H); <sup>13</sup>C NMR (CDCl<sub>3</sub>, 100 MHz) 172.53, 171.86, 155.63, 137.26, 136.76, 115.84, 115.71, 79.99, 53.84, 52.31, 51.63, 31.42, 29.63, 29.35, 28.28, 28.26; MS (FAB) *m/z* (relative intensity, %) 355.2 (MH<sup>+</sup>, 80), 299.2 (100), 255.2 (90), 243.2 (20). Anal. Calcd for C<sub>18</sub>H<sub>30</sub>N<sub>2</sub>O<sub>5</sub>: C, 61.00; H, 8.53; N, 7.90. Found: C, 60.78; H, 8.74; N, 7.82.

**(3S,10S)-(6E)-10-((*N*-*tert*-Butoxycarbonyl)amino)-3-methoxycarbonyl-2-azacyclodec-6-en-1-one (21).** To 500 mL of degassed CH<sub>2</sub>Cl<sub>2</sub> at reflux was added (PCy<sub>3</sub>)<sub>2</sub>Cl<sub>2</sub>Ru benzylidene (35 mg, 0.042 mmol). To this light purple solution at reflux was added a solution of **20** in degassed CH<sub>2</sub>Cl<sub>2</sub> (10 mL) via cannula. The purple color immediately faded to orange, and the reaction was allowed to reflux for 18 h. The reaction mixture was then exposed to air until black, and the solvent was removed under vacuum to afford a black solid. Flash chromatography (20% acetone/hexanes) afforded **21** as an off-white solid (62.2 mg, 68%). mp 132–133 °C (EtOAc/hexanes); *R*<sub>f</sub>: 0.28 (40% EtOAc/hexanes); IR (CH<sub>2</sub>Cl solution)  $\nu$  1739.4, 1734.1, 1729.8, 1723.1, 1718.2, 1700.6; <sup>1</sup>H NMR (CDCl<sub>3</sub>, 500 MHz)  $\delta$  6.54 (d, 1H, *J* = 10.0 Hz), 5.39 (m, 2H), 4.92 (bs, 1H), 4.79 (ddd, 1H, *J* = 12.1, 10.1, 2.4 Hz), 4.21 (bs, 1H), 3.70 (s, 3H), 2.44 (m, 1H), 2.32 (m, 1H), 2.18 (m, 2H), 2.06 (ddq, 1H, *J* = 14.5, 5.2, 2.6 Hz), 2.0 (m, 1H), 1.71 (m, 1H), 1.59 (dtd, 1H, *J* = 14.7, 12.1, 3.1 Hz), 1.48 (s, 9H); MS (FAB) *m/z* (relative intensity, %) 327.2 (MH<sup>+</sup>, 70), 307.1 (40), 271.1 (100). Anal. Calcd for C<sub>16</sub>H<sub>26</sub>N<sub>2</sub>O<sub>5</sub>: C, 58.88; H, 8.03; N, 8.58. Found: C, 58.87; H, 7.96; N, 8.58.

**(3S,10S)-(6E)-10-((2S)-2-((*N*-*tert*-Butoxycarbonyl)phenylalanyl)-amino-3-methoxycarbonyl-2-azacyclodec-6-en-1-one (22).** To **21** (56

mg, 0.17 mmol) in CH<sub>2</sub>Cl<sub>2</sub> (5 mL) at 0 °C was added Et<sub>3</sub>SiH (0.03 mL, 0.17 mmol). TFA (1 mL) was added, and the clear yellow solution was warmed to room temperature and stirred for 2 h. The reaction mixture was concentrated under reduced pressure and dried under vacuum for 24 h. The crude amine salt was taken up in CH<sub>2</sub>Cl<sub>2</sub> (5 mL) at room temperature and Boc-Phe-ONa (73.2 mg, 0.26 mmol) was added, followed by DIEA (0.09 mL, 0.51 mmol). To this homogeneous solution was added PyBop (132 mg, 0.26 mmol). After 1 h at room temperature, a fine white precipitate developed. Stirring was continued under Ar overnight, after which the reaction mixture was concentrated to a white solid. The residue was taken up in EtOAc (20 mL) and washed consecutively with 5% KHSO<sub>4</sub> (10 mL), 5% NaHCO<sub>3</sub> (10 mL), and brine (10 mL) and dried over Na<sub>2</sub>SO<sub>4</sub>. The organics were then filtered and concentrated to yield a solid which, upon flash chromatography (45:50:5 EtOAc/hexanes/MeOH) afforded **22** (61.5 mg 76%). *R*<sub>f</sub>: 0.28 (40% EtOAc/hexanes); mp: 168–170 °C (EtOAc/hexanes); [ $\alpha$ ]<sub>D</sub><sup>25</sup> +27.7° (*c* = 1.0, CHCl<sub>3</sub>); RP-HPLC Whatman ODS2 C-18 70:30 ACN:H<sub>2</sub>O(0.1% TFA) *t*<sub>R</sub> = 6.86 min; IR (CHCl<sub>3</sub> solution)  $\nu$  3428.6, 3009.8, 1738.2, 1686.1, 1680.6, 1497.9; <sup>1</sup>H NMR (CDCl<sub>3</sub>, 500 MHz)  $\delta$  7.26–7.36 (m, 5H), 6.66 (d, 1H, *J* = 7.3 Hz), 6.35 (d, 1H, *J* = 9.7 Hz), 5.34 (ddd, 1H, *J* = 15.0, 11.2, 3.1 Hz), 5.16 (ddd, 1H, *J* = 14.1, 10.6, 2.9 Hz), 4.99 (d, 1H, *J* = 5.9 Hz), 4.74 (ddd, 1H, *J* = 11.9, 10.07, 2.20 Hz), 4.52 (ddd, 1H, *J* = 8.24, 4.94, 2.93 Hz), 4.40 (X of ABX, 1H, *J*<sub>AX</sub> = 6.6, *J*<sub>BX</sub> = 7.5, *J*<sub>NHX</sub> = 5.9 Hz), 3.70 (s, 3H), 3.16 (AB of ABX, 2H, *J*<sub>AB</sub> = 14.3, *J*<sub>AX</sub> = 6.6, *J*<sub>BX</sub> = 7.5 Hz), 2.42 (tt, 1H, *J* = 14.1, 3.5 Hz), 2.25 (m, 1H), 2.11 (m, 2H), 1.99 (m, 1H), 1.85 (tdd, 1H, *J* = 13.9, 11.0, 3.1 Hz), 1.55 (m, 2H), 1.44 (s, 9H); <sup>13</sup>C NMR (CDCl<sub>3</sub>, 125 MHz) 172.18, 171.66, 171.24, 156.53, 136.52, 131.61, 129.13, 129.05, 128.12, 127.35, 81.10, 56.40, 52.90, 52.28, 51.65, 37.27, 31.32, 30.33, 29.81, 28.36 28.34; MS (FAB) *m/z* (relative intensity, %) 474.1 (MH<sup>+</sup>, 100), 418.1 (95), 374.1 (50), 308 (50); HRMS calcd for C<sub>25</sub>H<sub>36</sub>N<sub>3</sub>O<sub>6</sub>: 474.2605, found 474.2604. Anal. Calcd for C<sub>25</sub>H<sub>35</sub>N<sub>3</sub>O<sub>6</sub>: C, 63.40; H, 7.45; N, 8.87. Found: C, 63.22; H, 7.55; N, 8.52.

**(3S,10S)-(6E)-10-((S)-2-((*N*-*tert*-Butoxycarbonyl)phenylalanyl)-amino-3-(S)-methionamide)carboxy-2-azacyclodec-6-en-1-one (23).** Compound **22** (24 mg, 0.05 mmol) was dissolved in MeOH (5 mL) and cooled to 0 °C. A 0.25 N solution of NaOH (0.4 mL, 0.10 mmol) was slowly added. The reaction mixture was slowly warmed to room temperature and stirred for 8 h. After the disappearance of starting material was noted by TLC the reaction mixture was concentrated to a turbid suspension. The suspension was extracted 3 × 10 mL with EtOAc, the organic layers were dried over Na<sub>2</sub>SO<sub>4</sub>, filtered, and concentrated to a clear film. After drying overnight under vacuum, the film was dissolved in CH<sub>2</sub>Cl<sub>2</sub> (5 mL) and L-methionamide hydrochloride (13.8 mg, 0.075 mmol) was added. DMF (0.2 mL) was added to solubilize the methionine. DIEA (0.03 mL, 0.15 mmol), and PyBop (31.2 mg, 0.06 mmol) were added. The reaction was stirred overnight and then concentrated to a white solid. The solid was taken up in EtOAc (10 mL) and washed consecutively with 5% KHSO<sub>4</sub> (5 mL), 5% NaHCO<sub>3</sub> (5 mL), and brine (5 mL) and dried over Na<sub>2</sub>SO<sub>4</sub>. After filtering and concentrating, flash chromatography (5% MeOH/CH<sub>2</sub>Cl<sub>2</sub>) afforded a white solid that was recrystallized from EtOAc/petroleum ether to give **23** (75%) of **23**. mp 194–195.5 °C; *R*<sub>f</sub>: 0.35 (7% MeOH/CHCl<sub>3</sub>); *t*<sub>R</sub> = 14.81 min (70:30, MeOH/H<sub>2</sub>O, 0.1% TFA); <sup>1</sup>H NMR (DMF-*d*<sub>6</sub>, 500 MHz)  $\delta$  8.25 (d, 1H, *J* = 6.0 Hz), 7.68 (d, 1H, *J* = 7.9 Hz), 7.43 (br s, 2H), 7.21–7.34 (m, 6H), 7.11 (br s, 1H), 7.08 (d, 1H, *J* = 7.5 Hz), 5.61 (ddd, 1H, *J* = 13.5, 10.6, 1.8 Hz), 5.25 (ddd, 1H, *J* = 14.1, 10.4, 1.8 Hz), 4.59 (ddd, 1H, *J* = 11.2, 9.7, 1.7 Hz), 4.51 (ddd, 1H, *J* = 9.7, 7.5, 4.6 Hz), 4.42 (ddd, 1H, *J* = 7.6, 4.6, 3.2 Hz), 4.34 (dt, 1H, *J* = 7.6, 4.1 Hz), 3.21 (dd, 1H, *J* = 14.3, 4.4 Hz), 2.99 (dd, 1H, *J* = 14.1, 10.0 Hz), 2.51 (m, 1H), 2.38 (m, 1H), 2.26 (m, 2H), 2.02–2.08 (m, 7H), 1.91 (dtd, 1H, *J* = 13.9, 9.2, 5.3 Hz), 1.65 (m, 2H), 1.36 (s, 9H); <sup>13</sup>C NMR (DMF-*d*<sub>6</sub>, 125 MHz) 173.8, 173.6, 172.8, 172.3, 157.0, 139.1, 133.2, 129.9, 128.9, 128.5, 126.9, 79.3, 56.7, 54.8, 53.4, 52.9, 37.5, 33.0, 32.4, 30.5, 30.4, 28.7, 28.5, 28.4, 15.0; MS (FAB) *m/z* (relative intensity, %) 628 (MK<sup>+</sup>, 40), 612 (MNa<sup>+</sup>, 40), 590 (MH<sup>+</sup>, 70), 490 (50), 386 (100), 342 (60); HRMS calcd for C<sub>29</sub>H<sub>45</sub>N<sub>5</sub>O<sub>6</sub>S 590.3009, found 590.3012. Anal. Calcd for C<sub>29</sub>H<sub>44</sub>N<sub>5</sub>O<sub>6</sub>S: C, 59.06; H, 7.35; N, 11.87; S, 5.44. Found: C, 58.66; H, 7.59; N, 11.61; S, 5.32.

**(3S,10S)-(6E)-10-((S)-((N-tert-Butoxycarbonyl)alanyl)-(S)-phenylalanyl)amino-3-methoxycarbonyl-2-azacyclodec-6-en-1-one (24).** Compound **24** was prepared from **21** and Boc-Ala-Phe-OH in a manner analogous to **22** (51 mg, 55%); <sup>1</sup>H NMR (CD<sub>2</sub>Cl<sub>2</sub>, 500 MHz) δ 7.20–7.40 (m, 5H), 6.97 (d, 1H, *J* = 9.3 Hz), 6.87 (d, 1H, *J* = 8.1 Hz), 6.73 (d, 1H, *J* = 4.9 Hz), 5.48 (ddd, 1H, *J* = 14.6, 11.1, 2.2 Hz), 5.31 (dddd, 1H, *J* = 14.8, 10.6, 3.8, 1.7 Hz), 5.14 (d, 1H, *J* = 2.8 Hz), 4.67 (ddd, 1H, *J* = 11.7, 9.7, 2.0 Hz), 4.94 (X of ABX 1H, *J*<sub>NX</sub> = 4.9, *J*<sub>AX</sub> = 7.1, *J*<sub>BX</sub> = 4.1 Hz), 4.45 (ddd, 1H, *J* = 8.1, 5.1, 3.1 Hz), 4.02 (dq, 2H, *J* = 7.3, 3.7 Hz), 3.69 (s, 3H), 3.14 (AB of ABX 2H, *J*<sub>AB</sub> = 14.4, *J*<sub>AX</sub> = 7.1, *J*<sub>BX</sub> = 4.9 Hz), 2.49 (tdd, 1H, *J* = 14.3, 10.6, 3.7 Hz), 2.38 (tt, 1H, *J* = 14.1, 3.5 Hz), 2.31 (m, 1H), 2.38 (tdd, 1H, *J* = 13.5, 11.0, 2.7 Hz), 2.0 (m, 1H), 1.96 (ddq, 1H, *J* = 14.1, 4.8, 2.4 Hz), 1.72 (tdd, 1H, *J* = 14.5, 12.3, 2.8 Hz), 1.52 (ddt, 1H, *J* = 13.9, 4.8, 3.1 Hz), 1.36 (s, 9H), 1.33 (d, 3H, *J* = 7.1 Hz); <sup>13</sup>C NMR (CD<sub>2</sub>Cl<sub>2</sub>, 125 MHz) 174.4, 172.4, 172.0, 170.3, 156.1, 136.0, 132.2, 129.1, 128.9, 128.0, 127.5, 81.0, 55.0, 53.9, 53.4, 52.2, 52.0, 36.4, 32.1, 30.1, 29.2, 27.8, 27.1, 17.2; MS (Type: FAB) *m/z* (relative intensity, %) 545.2 (MH<sup>+</sup>, 30), 489.2 (25), 445.2 (20), 386.2 (20), 338.3 (25), 284.3 (15), 227.1 (32), 199.2 (20), 120.0 (100); HRMS calcd for C<sub>28</sub>H<sub>41</sub>N<sub>4</sub>O<sub>7</sub> 545.2974, found 545.2975.

**(3S,10S)-(6E)-10-((S)-((N-tert-Butoxycarbonyl)phenylalanyl)amino-3-((S)-carboxymethylphenylalanyl)carboxy-2-azacyclodec-6-en-1-one (25a).** Compound **25a** was prepared from **22** and L-phenylalanine in a manner analogous to **23** (44 mg, 79%). Crystallized from EtOAc/hexanes, mp 114–115 °C; *R*<sub>f</sub>: 0.34 (70% EtOAc/hexanes); <sup>1</sup>H NMR (CD<sub>2</sub>Cl<sub>2</sub>, 500 MHz) δ 7.19–7.39 (m, 5H), 6.78 (d, 1H, *J* = 7.9 Hz), 6.70 (d, 1H, *J* = 5.3 Hz), 6.58 (d, 1H, *J* = 7.9 Hz), 5.30 (2H, m), 4.98 (d, 1H, *J* = 2.6 Hz), 4.70 (dt, 1H, *J* = 7.5, 5.5 Hz), 4.41 (ddd, 1H, *J* = 11.5, 9.2, 1.8 Hz), 4.32 (ddd, 1H, *J* = 6.6, 5.1, 2.9 Hz), 4.20 (ddd, 1H, *J* = 8.4, 4.9, 3.7 Hz), 3.69 (s, 3H), 2.36 (tdd, 1H, *J* = 14.4, 7.3, 4.0 Hz), 2.28 (m, 1H), 2.15–2.20 (m, 2H), 2.05 (m, 1H), 1.94 (m, 1H), 1.62 (ddt, 1H, *J* = 14.4, 7.3, 3.4 Hz), 1.50 (ddd, 1H, *J* = 14.9, 12.7, 2.9 Hz), 1.48 (s, 9H); <sup>13</sup>C NMR (CD<sub>2</sub>Cl<sub>2</sub>, 125 MHz) 173.05, 172.04, 171.90, 171.58, 157.33, 136.94, 136.39, 133.23, 129.70, 129.37 (2C), 128.79, 127.82, 127.79, 127.08, 81.71, 57.46, 54.94, 53.87, 53.80, 52.47, 38.34, 37.60, 32.22, 29.26, 29.21, 28.98, 28.50; MS (Type: FAB) *m/z* (relative intensity, %) 659 (MK<sup>+</sup>, 20), 643 (MNa<sup>+</sup>, 20), 621 (MH<sup>+</sup>, 20), 605 (20), 521 (20), 386 (40), 358 (35), 342 (20), 180 (60), 120 (100); HRMS calcd for C<sub>34</sub>H<sub>44</sub>N<sub>4</sub>O<sub>7</sub> 621.3290, found 621.3288.

**(3S,10S)-(6E)-10-((S)-((N-tert-Butoxycarbonyl)alanyl)-(S)-phenylalanyl)amino-3-((S)-carboxymethylphenylalanyl)carboxy-2-azacyclodec-6-en-1-one (25b).** Compound **25b** was prepared from **24** and L-phenylalanine in a manner analogous to **23** (48 mg, 78%). <sup>1</sup>H NMR (CD<sub>2</sub>Cl<sub>2</sub>, 750 MHz) δ 7.15–7.40 (m, 10H), 6.97 (d, 1H, *J* = 7.0 Hz), 6.96 (d, 1H, *J* = 9.5 Hz), 6.87 (d, 1H, *J* = 7.9 Hz), 6.71 (d, 1H, *J* = 5.5 Hz), 5.47 (ddd, 1H, *J* = 14.5, 11.1, 2.1 Hz), 5.27 (dddd, 1H, *J* = 15.0, 11.0, 3.6, 1.6 Hz), 5.12 (d, 1H, *J* = 2.7 Hz), 4.67 (X of ABX 1H, *J*<sub>NX</sub> = 7.9, *J*<sub>AX</sub> = 5.5, *J*<sub>BX</sub> = 7.6 Hz), 4.36 (ddt, 1H, *J* = 11.7, 9.5, 2.2 Hz), 4.35 (ddd, 1H, *J* = 7.1, 3.3, 4.5 Hz), 4.27 (X of ABX 1H, *J*<sub>NX</sub> = 4.6, *J*<sub>AX</sub> = 7.1, *J*<sub>BX</sub> = 4.9 Hz), 3.98 (dq, 2H, *J* = 7.2, 2.7 Hz), 3.66 (s, 3H), 3.14 (AB of ABX 2H, *J*<sub>AB</sub> = 14.4, *J*<sub>AX</sub> = 7.1, *J*<sub>BX</sub> = 4.9 Hz), 3.03 (AB of ABX 2H, *J*<sub>AB</sub> = 13.9, *J*<sub>AX</sub> = 5.5, *J*<sub>BX</sub> = 7.6 Hz), 2.60 (tdd, 1H, *J* = 14.3, 11.6, 3.4 Hz), 2.31 (tt, 1H, *J* = 14.4, 4.4 Hz), 2.28 (m, 2H), 2.08 (tdd, 1H, *J* = 14.5, 4.9, 2.6 Hz), 2.0 (m, 2H), 1.34 (s, 9H), 1.33 (d, 3H, *J* = 7.3 Hz); <sup>13</sup>C NMR (CD<sub>2</sub>Cl<sub>2</sub>, 125 MHz) 174.6, 173.0, 171.7, 171.6, 171.0, 156.4, 136.7, 135.7, 133.1, 129.4, 129.1, 129.0, 128.3, 127.9, 127.6, 126.6, 81.2, 55.4, 54.9, 53.5, 53.2, 52.6, 52.1, 38.1, 36.5, 32.5, 29.1, 28.7, 27.9, 27.2, 17.1; MS (Type: FAB) *m/z* (relative intensity, %) 692.3 (MH<sup>+</sup>, 20), 614 (25), 592.3 (30), 515.3 (25), 457.3 (30), 258.2 (100), 187 (70); HRMS calcd for C<sub>37</sub>H<sub>50</sub>N<sub>5</sub>O<sub>8</sub> 692.3662, found 692.3659.

**X-ray Crystallography for 21.** A suitable crystal was mounted using oil (Paratone-N, Exxon) to a thin glass fiber. The sample was bound by faces (1 0 -1), (-1 0 1), (1 0 1), (-1 1 0), (0 1 1), and (0 -1 -1). Distances from the crystal center to these facial boundaries were 0.010, 0.010, 0.080, 0.080, 0.190, and 0.190 mm, respectively. Crystal and refinement details are given in Table 12. Systematic conditions suggested the ambiguous/unambiguous space group P2(1). Standard intensities monitored during frame collection showed no decay; decay correction was not applied. Intensity data were reduced

**Table 12.** Crystallographic Data for **21**

empirical formula	C <sub>16</sub> H <sub>26</sub> N <sub>2</sub> O <sub>5</sub>	vol, Å <sup>3</sup>	1795.4(4)
formula mass	326.39	<i>Z</i>	4
crystal system	monoclinic	absorption coeffs	0.090 mm <sup>-1</sup>
space group	P2(1)	<i>T</i> (K)	198(2) K
<i>a</i> , Å	9.3911(11)	reflens collected	9469 [ <i>R</i> (int) = 0.1248]
<i>b</i> , Å	10.0489(12)	<i>R</i> indices (all data)	<i>R</i> 1 = 0.2603, <i>wR</i> 2 = 0.3714
<i>c</i> , Å	9.509(2)	goodness-of-fit on <i>F</i> <sup>2</sup>	1.151
α, deg	90	ρ <sub>calc</sub> , Mg/m <sup>3</sup>	1.207
β, deg	102.782(3)	μ, mm <sup>-1</sup>	0.090
γ, deg	90		

by 3d-profile analysis using SAINT and corrected for Lorentz-polarization effects and for absorption. Scattering factors and anomalous dispersion terms were taken from standard tables.<sup>64</sup> The structure was solved by direct methods;<sup>65</sup> the correct C, N, O atom positions were deduced from a vector/electron density map. Subsequent cycles of isotropic least-squares refinements followed by an unweighted difference Fourier synthesis revealed positions for the remaining non-H atoms. Methyl H atom positions, 4-CH~3~, were optimized by rotation about 2-C bonds with idealized C–H and H–H distances. Remaining H atoms were included as fixed idealized contributors. H atom U's were assigned as 1.2 times *U*<sub>eq</sub> of adjacent C atoms. Non-H atoms were refined with anisotropic thermal coefficients. Successful convergence of the full-matrix least-squares refinement on *F*<sup>2</sup> was indicated by the maximum shift/error for the last cycle. The highest peaks in the final difference Fourier map were in the vicinity of the C, N, and O atoms; the final map had no other significant features. A final analysis of variance between observed and calculated structure factors showed no dependence on amplitude or resolution. Full details of the crystallographic results are included in the Supporting Information.

**Acknowledgment.** Support for this work was provided by the Eli Lilly Corporation and the National Institutes of Health (PHS 5R01 DK15556 and PHS 5R01 CA33091). We thank Prof. Peter A. Petillo and Dr. Howard Robinson for many helpful discussions and Dr. Bruce Gitter and Tiffanie Lamar for conducting the Substance P binding assays. Dr. Feng Lin and Dr. Vera Mainz of the University of Illinois Molecular Spectroscopy Lab are gratefully acknowledged for assistance in conducting NMR spectroscopic experiments and Dr. Scott Wilson and Teresa Prussak-Wieckowski for obtaining X-ray crystallographic data. NMR spectra were obtained in the Varian Oxford Instrument Center for Excellence in NMR Laboratory. Funding for this instrumentation was provided in part from the W. M. Keck Foundation, the National Institutes of Health (PHS 1 S10 RR104444-01), and the National Science Foundation (NSF CHE 96-10502). Mass spectra were obtained on instruments supported by grants from the National Institute of General Medical Sciences (GM 27029), the National Institutes of Health (RR 01575), and the National Science Foundation (PCM 8121494).

**Supporting Information Available:** <sup>1</sup>H and <sup>13</sup>C NMR spectra for compounds **11**, **13**, **14**, **22**, **24**, **25a** (Figures S1–S12); Tables S1–S6 listing full crystallographic information, atomic coordinates, anisotropic displacement parameters, and intramolecular bond distances and angles; complete ORTEP plots for compound **21** (Figures S13–S15), and complete experimental procedures and characterization for compounds **6–9**, **11–15**, **24**, **25a**, and **25b** (S16–S22) (35 pages). See any current masthead page for ordering information and Web access instructions.

JA974023Y

(64) Wilson, A. J. C. *International Tables for X-ray Crystallography*; Wilson, A. J. C., Ed.; Kluwer Academic Publishers: Dordrecht, 1992; Vol. C, pp 500–502, 219–222.

(65) Sheldrick, G. M. *Acta Crystallogr.* **1990**, *A46*, 467–473.